

# Which is the Dynamics of Stretched Biomolecular Chains?

Vincenzo Villani

*Dipartimento di Chimica dell'Università della Basilicata*

*Via N. Sauro, 85*

*85100 Potenza (Italy)*

[villani@unibas.it](mailto:villani@unibas.it)

*Today speaking on sciences describing nature is always, in some ways, speaking on symmetries (and about symmetry breaking) (E. Castellani, Simmetria e Realtà, 'Le Scienze quaderni', n. 118, February 2001)*

---

Internet Electronic Conference of Molecular Design 2003, November 23 – December 6

## Abstract

**Motivation.** The *pulled chain-ends problem*, where external forces are applied at both ends of a linear chain, is of general interest in the behavior of macromolecules in rubber networks, during the elastic deformation process. In particular, the present work is addressed to shed an insight to the constrained dynamics of elastic repeat motif of Elastin, the rubber protein of vertebrates, interesting also as a biomaterial in medicine. Four models with external forces for the hydrated Elastin flexible sequence **Gly-Leu-Gly-Gly** have been developed. The free molecule represents the *chain in the relaxed state of the elastomeric network* (unperturbed model) in fact, on microscopic length scales individual chains move essentially freely as in a polymer solution. The forced ones model the *chain in the elastin strained states* (stretched models). The applied constraints take implicitly into account the effect transmitted down to both the ends inside the stressed polymer network. In such a way the attention is focused to the internal changes induced in the stretched chain.

**Method.** In this framework the tetrapeptide *Ac-Gly-Leu-Gly-Gly-NMe* has been modeled in aqueous solution by nearly 10 ns of MD on parallel computers. The chain dynamics was carefully analyzed in terms of probability density distributions, time correlation functions, fast Fourier transforms, Hurst critical exponent, according to the classical theory of the rubber elasticity. The end-to-end distance and the gyration radius describing conformational motions, the mass-center displacement describing translational motions and the configurational 3N-dimensional vector  $\mathbf{R}_q$ , whose components are the Cartesian coordinates of chain atoms, describing the global motion of the peptide was considered.

**Results.** In all cases an anomalous diffusion with  $H < 1/2$ , typical of the fractional Brownian motions of Self-Organized Criticality in *poor-solvent* solution, has been observed. The global mobility of unstrained or strained chains is similar, although due to strongly different effects. In fact, in the unperturbed system the motion is equidistributed among all internal degree-of-freedom, in contrast, on stretching, the symmetry breaking of the internal motions is observed and the dynamics concentrates in the few slower collective modes with large fluctuations of the mass-center. This behavior typical of nonlinear complex systems is at the basis of the formation of self-organized structures.

**Conclusions.** The proposed *mechanism of Chaos-Symmetry-Breaking*, in agreement with the previous *mechanism of Transition-to-Chaos* would be at the basis of the entropic drop and retractile force of the stressed rubber network. As expected, the entropy change in the proposed mechanism is proportional to the density of the cross-links in agreement with the elasticity experiments and theory.

**Availability.** <http://amber.scripps.edu/>, <http://www.trusoft.netmegs.com/benoit.html>, <http://www.mpiPKS-dresden.mpg.de/~tisean/>

**Keywords.** Molecular Dynamics Simulations; Biomaterials; Protein Rubbers; Time Series Nonlinear Analysis; Chaos; Theory of Rubber Elasticity.

---

## Abbreviations and notations

MD, Molecular Dynamics Simulations

RW, Random Walks

FBW, Fractional Brownian Walks

SOC, Self-Organized Criticality

BW, Brownian Walks

## 1 INTRODUCTION

*The most important question of the rubber elasticity is how the macroscopic deformation of the network is transmitted down to the individual chains*<sup>1</sup>. In other words, *which is the dynamics of strained chains in rubber networks?*

Generally, the rubber deformation occurs at a constant volume, and, in the case of the simple uniaxial elongation, we observe a compensating contraction along the directions orthogonal to that of stretching. According to the rubber molecular theories of elasticity<sup>2,3</sup>, to such macroscopic modifications, the variation of the density distribution of the cross-linked chain end-to-end distances corresponds at a microscopic level. The mean value distribution is shifted to higher values along the stretch axis and to lower ones along the orthogonal axes, with respect to the unperturbed values. The extent of the mean value and the fluctuations amplitude changes remain controversial<sup>4</sup>. In the classical theories, the microscopic affine deformation and the conservation of the isotropic Brownian motion of the chain are assumed for small deformations.

In the present work, the deformed state of an Elastin polypeptide has been represented by elongated chains, constrained at the ends through a harmonic potential, simulating a stretched chain as in Wasserman-Salemme<sup>5</sup> and Li-Alonso-Bennion-Daggett<sup>6</sup> works about elastin-based biopolymers as the Urry's polypentapeptide  $(VPGVG)_n$ .

If we imagine pulling a flexible *phantom chain* at both ends<sup>7</sup>, then the symmetry due to thermal agitation is broken and the free energy  $A$  is given by

$$A = 3kTR^2/2R_0^2 \quad (1.1)$$

and the elastic force arises

$$F = - 3kT R/R_0^2 \quad (1.2)$$

where  $\mathbf{R}$  is the end-to-end vector,  $kT$  the thermal energy factor and  $R_0^2$  the mean square end-to-end distance. These are the fundamental formula of ideal chains.

The free energy per unit volume of an ideal rubber network is obtained through the generalization of paste equations and reads

$$A = 3\nu kT \langle R^2/R_0^2 \rangle / 2 \quad (1.3)$$

where the average is over  $\nu$  crosslinked chains. For a generic constant volume deformation, in the classical *affine* assumption, we can write the *constitutive equation of ideal rubber*

$$A = \nu kT (\lambda_1^2 + \lambda_2^2 + \lambda_3^2) / 2 \quad (1.4)$$

For the uniaxial deformation the constitutive equation becomes

$$A = \nu kT (\lambda^2 + 2/\lambda) / 2 \quad (1.5)$$

and the *engineering stress*  $\sigma$  and *true stress*  $\Sigma$  read:

$$\sigma = \nu kT (\lambda - 1/\lambda^2) \quad (1.6)$$

$$\Sigma = \nu kT (\lambda^2 - 1/\lambda) \quad (1.7)$$

Two basic complex behaviors are ignored by the classical theory of rubber elasticity: the *finite extensibility* of the chains and the *entanglements*. The so-called *Mooney effect*, from the ratio plot  $\sigma_{exp}/\sigma$  vs.  $\lambda^{-1}$ , is due to both simplifications.

In Elastin, different repeating sequences are present, some of which seem to have an important role in the elasticity mechanism<sup>8</sup>. The peptide *Ac-Gly-Leu-Gly-Gly-NMe* whose dynamic behavior is analyzed, is one of the better-studied repeating sequences.

The glycine-rich hydrophobic segments have been in-depth studied both experimentally and through Molecular Modeling<sup>9-16</sup>. Nevertheless, the behavior of folded or extended conformations in the presence of external forces applied at the end-groups, have been only marginally examined, although the polypeptide chain in the protein experiences them in correspondence of the deformed states, according to the rubber elasticity theories. MD of the glycine-rich tetrapeptide *Ac-Gly-Leu-Gly-Gly-NMe* in aqueous solution, applying external forces to the end-carbon atoms – *constrained chain-end models* – contribute to fill this gap.

The tetrapeptide was simulated in conditions of elongational deformation, by varying the force constant  $K$  of the harmonic potential applied to the peptide end-atoms. In this way, the applied

force constant was used as a *control parameter* through which different possible stretching conditions were simulated.

In the past<sup>12</sup>, we have hypothesized that the conformational changes, on passing from the stretched to the relaxed state, are accomplished by a dynamics transition: the relaxed state presents a diffusive-chaotic motion, while the stretched a vibrational-solitonic one. These states are characterized by a different entropy, higher for the relaxed than for the stretched state. This agrees with what expected for nonlinear systems, which can experience different kinds of motions, depending upon the oscillation amplitude. In fact the stretched state gives high frequency and low amplitude motions, and the application of an external force implies a decrease of the volume of the phase space accessible to the system. In contrast, the relaxed state can experience a larger region in the phase space, due to the larger amplitude motions. The results obtained for short sequences are thought to be extended to Elastin and it has been proposed the *Transition-to-Chaos mechanism*<sup>12</sup> for the elasticity and the *Soft-Solution model*<sup>17</sup> for the Rubber Protein morphology.

## 2 METHODS

Potential energy was calculated by the Cornell *et al.*<sup>18</sup> force field, where the energy partition is assumed, as a sum stretching, bending, dihedral, nonbonded pairs interactions terms.

The aqueous solution waters were explicitly considered, according to Jorgensen *et al.*<sup>19</sup> TIP3P model, in which the molecules are considered as rigid, and Lennard-Jones and electrostatic interaction taken into account.

In order the molecular system can be adequately treated it was necessary to take into account a realistic model, that in our case is a dilute aqueous solution of the *Ac-Gly-Leu-Gly-Gly-NMe* tetrapeptide in 852 water molecules at room conditions (300 K and 1 atm). The usual periodic boundary conditions were applied.

The MD at constant temperature and pressure by means of the method of Berendsen *et al.*<sup>20</sup> was accomplished by coupling the system to external baths by the time constants  $\tau_T = \tau_P = 0.2$  ps.

The motion equations were integrated in Cartesian coordinates by means of the Verlet leapfrog algorithm<sup>21</sup>. The integration step  $\delta t$  was set as 1 fs and the system trajectories sampled every  $\Delta t = 0.04$  ps.

To perform the constrained simulations the end carbon atoms strained by a harmonic force with a force constant  $K$  of  $100 \text{ kcal/mol}\text{\AA}^2$  (value corresponding to a bending deformation, e.g.  $K=80 \text{ kcal/mol deg}^2$  for N-C-O), 10 and 1 was considered.

Four models of the elastin polypeptides have been elaborated. The unperturbed state, without external forces, has been obtained starting from the results of a previous Simulated Annealing of the aqueous solution towards the normal conditions, as described in the literature<sup>13</sup>. A highly perturbed state has been considered by straining through an external harmonic force, having a force constant  $K = 100 \text{ kcal/mol\AA}^2$  the ends of the fully extended chains, extending a previously published simulation. This worst stretched case has been assumed as reference limit. Two cases of moderate stretching have been selected. The first has been obtained by constraining the final state of the unperturbed dynamics using  $K = 10$ ; the second constraining the final state of the previous dynamics using  $K = 1$ . In our intention, the free molecule represents the corresponding chain segment in the relaxed protein. In fact, in such conditions the protein chain, although crosslinked, behaves as a usual molecule in solution<sup>7</sup> and the tetrapeptide is enough long to be able to simulate the local mobility of the chain. In contrast, the strained and partially extended models represent possible chain states during the process of elastic deformation of the parent protein.

The system evolution has been analyzed by taking into account the about 200,000 points (nearly 10 ns) of the system trajectory stored during these simulations.

The dynamic behavior of the peptide in aqueous solution has been characterized by time series linear and nonlinear analysis methods of the following structural parameters: the end-to-end distance between the end-carbon atoms of the chain, the gyration radius, the displacement of the mass-center and the  $R_g$   $3N$ -dimensional configurational vector modulus. Its components are the Cartesian coordinates of each peptide atoms, whose modulus  $R_g$  has been considered through the extended Pythagorean theorem.

From the viewpoint of the end-to-end vector, the molecular detail is ignored and the system reduced to the dynamics of a vector, implicit function of the  $3N-6$  internal degrees-of-freedom. This variable describes the fluctuations of the crosslinks in the classical theories of the rubber elasticity. In the estimate of the gyration radius the molecular system is reduced to a spherical surface with the same inertial momentum, whose radius is a function of the internal variables.

From the configurational point of view, the system is reduced to the motion of the representative point in the  $3N$ -dimensional spatial section of the phase space.

Then, end-to-end distance and gyration radius take into account the internal dynamics and  $R_g$  takes into account the global dynamics of the examined system.

The Hurst exponent is a measure of the long-time correlations in a time series<sup>22</sup> and allows the classification of time series since it is able to distinguish the existence of correlations from random noise. In the *rescaled range analysis* or *R/S analysis*, the span of a random process is

divided by its variance, resulting in a new variable that depends on the length of the data recorded. Let us define the average of the time series  $L(t)$  over the time interval  $\tau$ .

$$\langle L \rangle_{\tau} = (\sum_{t=1}^{\tau} L(t)) / \tau \quad (2.1)$$

Let us also define *the accumulated departure*  $A(t, \tau)$  of  $L(t)$  from the mean as:

$$A(t, \tau) = \sum_{u=1}^t (L(u) - \langle L \rangle_{\tau}) \quad (2.2)$$

So that *the span of the process*  $S(\tau)$  is defined by:

$$S(\tau) = \max_{1 < t < \tau} A(t, \tau) - \min_{1 < t < \tau} A(t, \tau) \quad (2.3)$$

Let us also introduce *the standard expression for the variance*  $V(\tau)$ :

$$V(\tau) = (\sum_{t=1}^{\tau} (L(t) - \langle L \rangle_{\tau})^2 / \tau)^{1/2} \quad (2.4)$$

The rescaled Hurst analysis consists in studying the properties of the ratio:

$$R(\tau) = S(\tau) / V(\tau) \quad (2.5)$$

The dependence of  $R(\tau)$  on the number of data points follow an empirical *power law* described as  $R(\tau) = R_0 \tau^H$  obtained over a wide range of time lengths  $\tau$ , where  $0 < H < 1$  is the Hurst exponent. The *fractal dimension* of the trace can then be calculated from the relationship  $D = 2 - H$ .

If  $H = 1/2$  *Brownian motions* with short-range correlation occur. According to Mandelbrot<sup>22</sup>, processes with  $H = 1/2$  are defined *fractional* and show long-range correlations. *Fractional*

*Brownian motions* are divided into two families: if  $H > 1/2$ , the positive correlation among the increments of motion implies the *persistence* in the trajectory of the induced motion. In contrast, if  $H < 1/2$ , the anticorrelation on a large scale generates an *antipersistent* behavior.

The Power Spectrum method for estimation of Hurst exponent uses the properties of self-affine trace. In practice, to obtain an estimate of Hurst exponent, one calculates the power spectrum  $I(k)$ , where  $k$  is the wavenumber, and plots the logarithm of  $I(k)$  versus the logarithms of  $k$ . If the trace is self-affine, this plot should follow a straight line with a negative slope  $-\beta$ . This value is related to the Hurst exponent as  $\beta = 2H + 1$ .

It should be emphasized that obtaining an adequate estimate of the power spectrum of a sampled function is not a trivial matter. For example, one may take a Fourier transform of the input series using available fast Fourier transform algorithms and squaring the transform coefficients. This operation results in the periodogram, which is a poor estimate of the power spectrum. The principal defect of the periodogram is that the estimate of the power at any frequency is very noisy, with the amplitude of the noise being proportional to the spectral power. BENOIT offers an improved technique of spectral estimation where averaging periodograms obtained in equal logarithmic intervals of the data set smoothes this noise.

The time series are analyzed as time normalized autocorrelation functions, according to the following equation:

$$C_x(\tau) = \langle \Delta x(t) \Delta x(t + \tau) \rangle / \langle \Delta^2 x(t) \rangle \quad (3.1)$$

where  $x$  is the selected variable,  $\tau$  the correlation time and

$$\Delta x(t) = x(t) - \langle x(t) \rangle \quad (3.2)$$

$$\Delta^2 x(t) = [x(t) - \langle x(t) \rangle]^2 \quad (3.3)$$

This function gives an assessment of the dependence upon coupling among time neighboring points. The correlation time  $\tau_0$  defines the time when the correlation function assumes the value  $1/e$ .

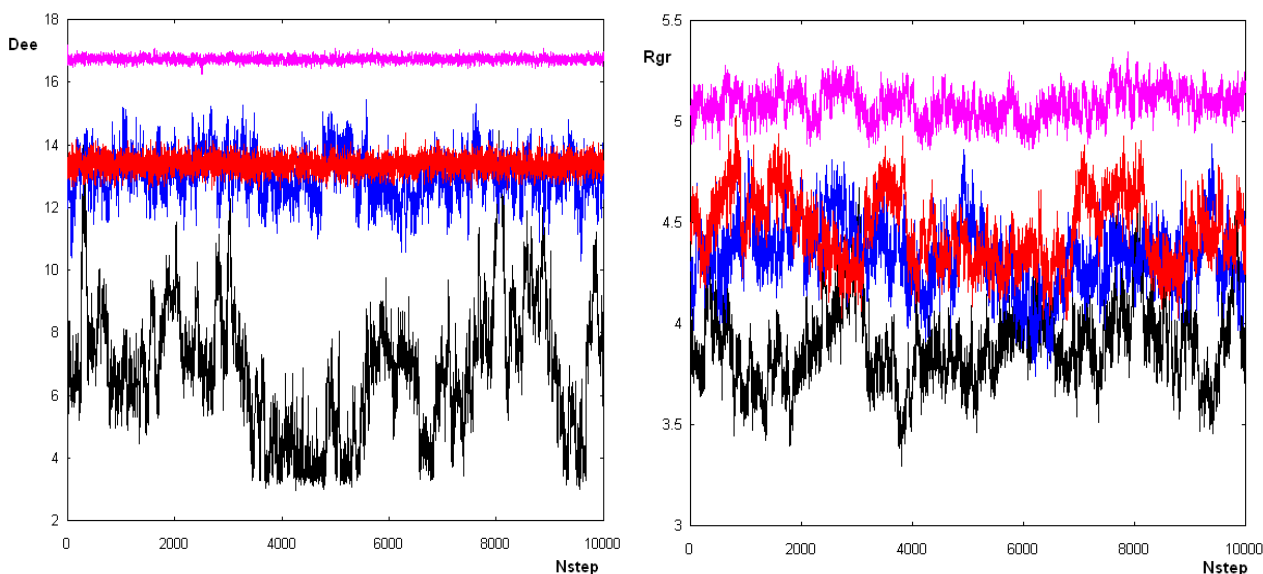
Highly random time series are not correlated: the correlation function goes abruptly to zero with a very short correlation time. Highly correlated data, as in harmonic vibrations, have oscillating correlation functions, with a slow varying trend. Chaos from nonlinear differential equations, as the motion equations of MD, can be correlated in a complex way.

## 2.1 Computer Software

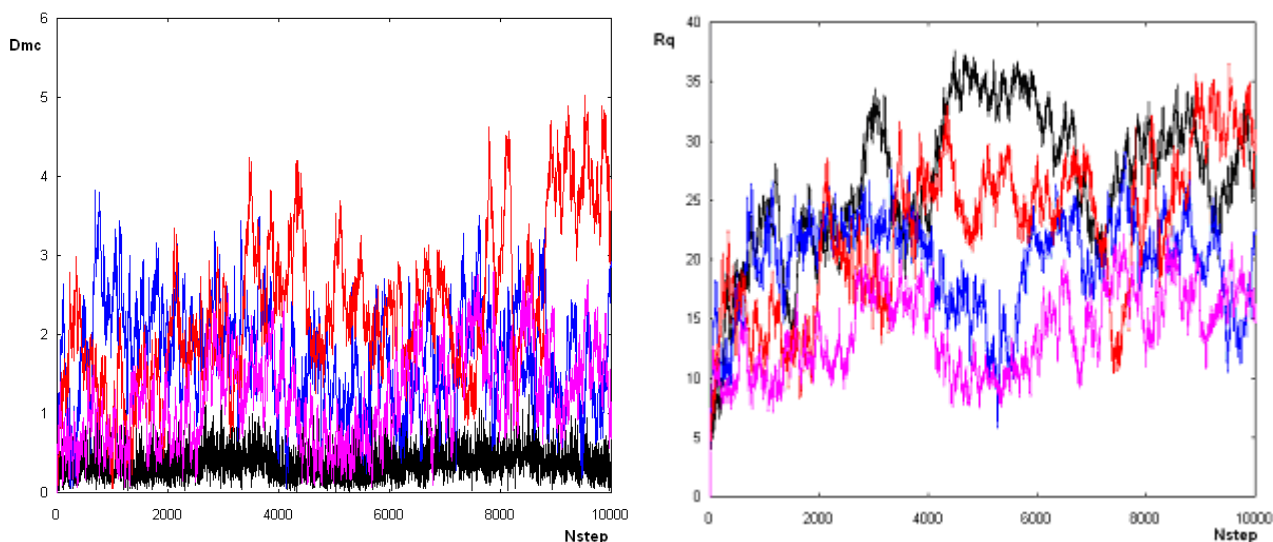
The MD was performed using the AMBER<sup>23</sup> software developed by Kollman *et al.*, under the UNIX operating system on a cluster of parallel computers. The data analysis has been carried out using BENOIT<sup>24</sup>, TISEAN<sup>25</sup> and homemade FORTRAN software.

## 3 RESULTS AND DISCUSSION

In **Fig. 1** the strong changes of the dynamics in the presence of the end-constraints are evident even from a qualitative examination of the trajectories of the different selected variables. In particular, as expected, the fluctuation amplitude of the end-to-end distance is inversely proportional to the intensity of the applied constrain and a similar, although less evident, trend is observed for the gyration radius. In contrast, in all cases, an increase in the mass-center displacement of the system is observed in the presence of external forces. Nevertheless, the system configurational mobility of the strained systems is lower or similar than that of the free one.

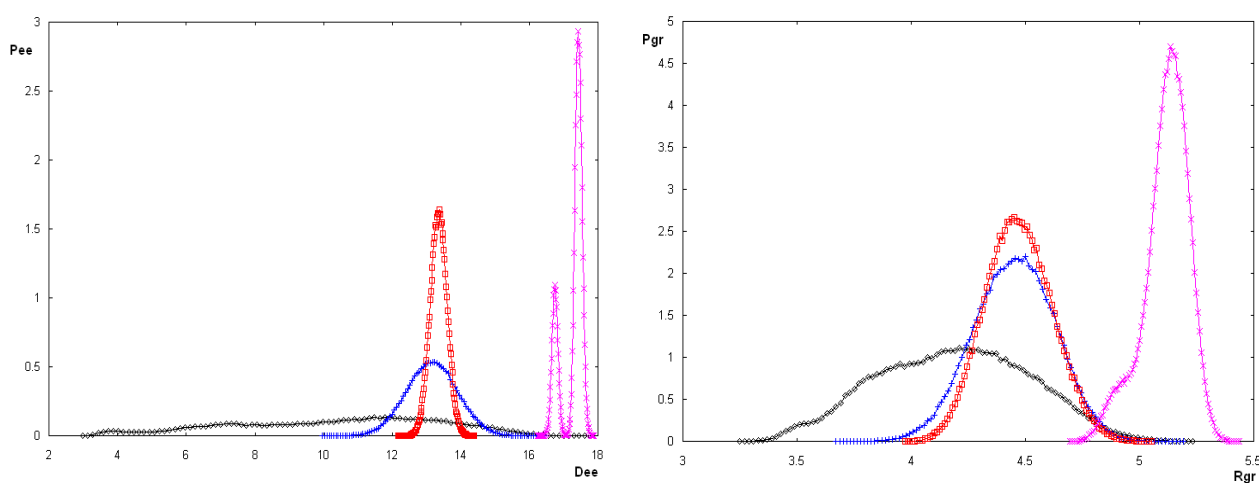






**Fig. 1** As in all the following figures, the black curve corresponds to the unperturbed model and colored curves to constrained ones: blue for  $K=1$  kcal/mol $\text{\AA}^2$ , red for  $K=10$  and violet for  $K=100$ .

The quantitative analysis of the previous observations is conducted in **Fig. 2**, where the distributions of the probability density  $P_x$  are shown, and in **Table 1**, where the mean and *rms* values of the selected variables are reported. In particular, the narrowing of the histograms of end-to-end distance is evident, on passing from the free to the forced system. In these last cases impressive Gaussian distributions are observed, typical of random highly uncorrelated motions. An analogous trend is observed for the histograms of the gyration radius. This is in agreement with the expected configurational entropy reduction of flexible chains on the elastic deformation. In contrast, the histograms of the mass-center displacement are always larger in the presence of external constrains. This is in agreement with the presence of *collective fluctuations* on the external force. Finally, the position and the amplitude of the  $R_q$  histograms,  $P_q$ , confirm that the global mobility, as well known, is invariant respect to the intensity of the applied constrains.



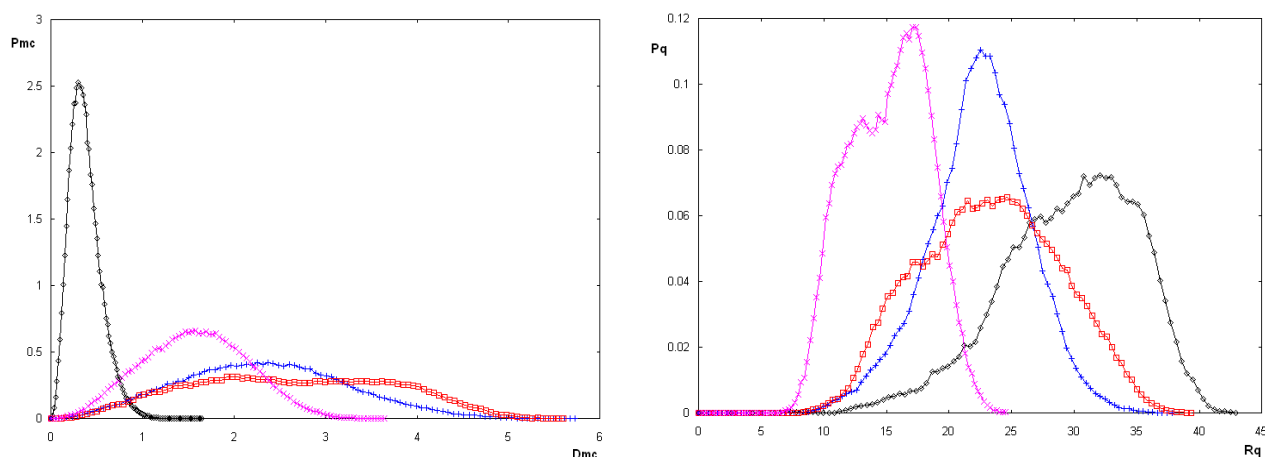


Fig. 2

| <b>K</b><br>average & rms | <b>0</b>      | <b>1</b>      | <b>10</b>     | <b>100</b>    |
|---------------------------|---------------|---------------|---------------|---------------|
| $D_{ee}$                  | 10.36<br>3.04 | 13.15<br>0.74 | 13.35<br>0.25 | 17.26         |
| $R_{gr}$                  | 4.19<br>0.33  | 4.45<br>0.18  | 4.47<br>0.15  | 5.11<br>0.10  |
| $D_{mc}$                  | 0.38<br>0.17  | 2.34<br>0.91  | 2.64<br>1.09  | 1.58<br>0.57  |
| $R_q$                     | 29.62<br>5.42 | 22.42<br>4.07 | 23.22<br>5.55 | 15.19<br>3.21 |

Table 1

A coherent picture emerges from the analysis of the correlation functions  $C_x(\tau)$  of **Fig. 3** and from the corresponding correlation times  $\tau_0$  of **Table 2**. In general, *in the presence of the applied external force, we observe a decrease of the correlation-symmetry of the internal and global functions and a corresponding increase of the collective fluctuations with the mass-center displacement*. In particular, the described trend is well evident in the case of  $C_{ee}(\tau)$ . For  $C_{gr}(\tau)$  a decrease in the symmetry of the forced models with respect to the free ones is observed, nevertheless no significant differences are obtained between the forced cases with  $K=1$  or 10. Moreover the high correlation for  $K=100$  is anomalous. Likely, in this last case, being frozen the internal motions, external rotational motions take place. In the  $R_q$  correlation functions,  $C_q(\tau)$ , the several motions interfere, evidencing the maximum correlation in the unperturbed model, essentially ruled by the independent internal motions, and collective effects for  $K=10$  and 100.

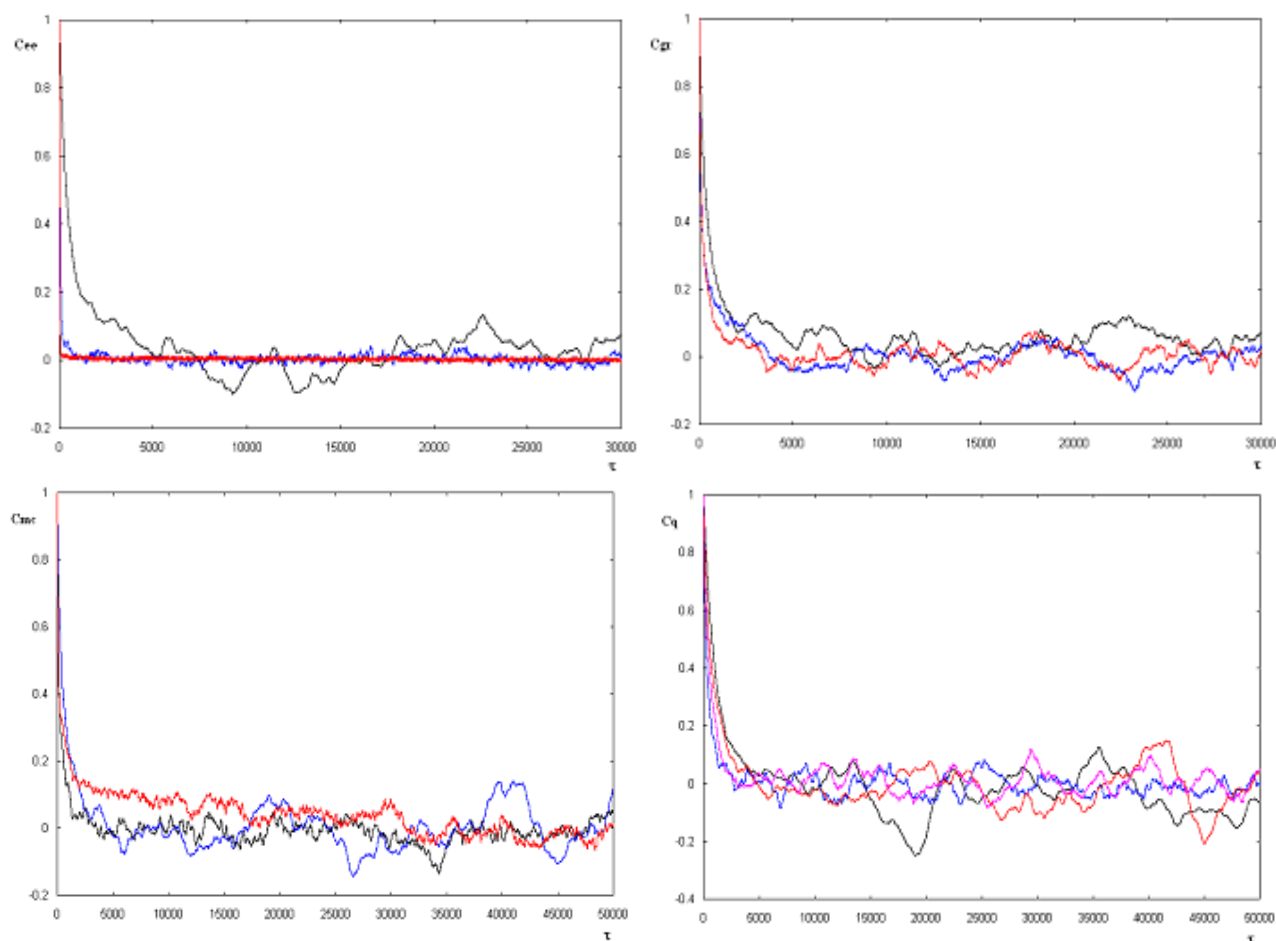


Fig. 3

| $K \backslash \tau_0$ | 0    | 1   | 10  | 100  |
|-----------------------|------|-----|-----|------|
| $D_{ee}$              | 570  | 29  | 2   | 1    |
| $R_{gr}$              | 502  | 157 | 167 | 1425 |
| $D_{mc}$              | 2    | 208 | 603 | 222  |
| $R_q$                 | 1094 | 342 | 828 | 598  |

Table 2

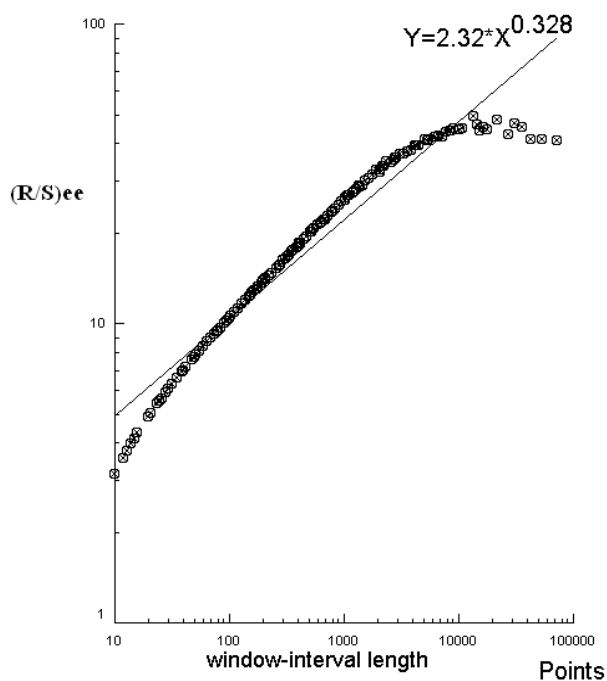


Fig. 4

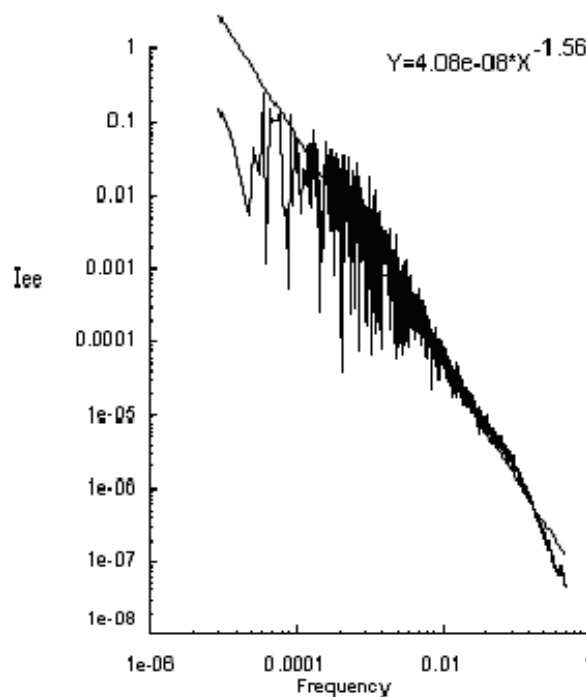


Fig. 5

| <b>K</b><br><b>H</b>  | <b>0</b> | <b>1</b> | <b>10</b> | <b>100</b> |
|-----------------------|----------|----------|-----------|------------|
| <i>D<sub>ee</sub></i> | 0.33     | 0.18     | 0.1       | 0.1        |
| <i>R<sub>gr</sub></i> | 0.41     | 0.38     | 0.39      | 0.34       |
| <i>D<sub>mc</sub></i> | 0.13     | 0.36     | 0.37      | 0.30       |
| <i>R<sub>q</sub></i>  | 0.41     | 0.38     | 0.39      | 0.34       |

Table 3

| <b>K</b><br><b>H</b>  | <b>0</b> | <b>1</b> | <b>10</b> | <b>100</b> |
|-----------------------|----------|----------|-----------|------------|
| <i>D<sub>ee</sub></i> | 0.27     | 0        | 0         | 0          |
| <i>R<sub>gr</sub></i> | 0.20     | 0        | 0         | 0          |
| <i>D<sub>mc</sub></i> | 0        | 0.38     | 0.39      | 0.26       |
| <i>R<sub>q</sub></i>  | 0.36     | 0.35     | 0.38      | 0.30       |

Table 4

In Fig. 4 – Table 3 and Fig. 5 – Table 4 the outcome of Hurst exponent estimation of the time series by R/S and Power spectrum analysis are reported, respectively. The previous conclusions are confirmed in an evident way: the free chain possesses uncorrelated conformational mobility, the

end-constrained models concentrate their mobility in collective motions with mass-center fluctuations. Globally the mobility of the free or strained chains is similar, but due to different origins. This, as previously said, has deep implications on the entropic changes, which occur in the presence of constrains, and is in agreement with the experimentally observed entropy loss in elastic macromolecules upon stretching. In other words, the conformational variables of the unperturbed system, show the character of Fractional Brownian Motions with  $0 < H < 0.5$ , dynamics which is typical of SOC<sup>26</sup> and chaotic, under the percolation threshold, systems. In the constrained systems, the variables have the character of RW with  $H=0$ . As largely discussed elsewhere, this behavior is the resultant of the linear dynamics of the normal modes of vibration for a number of independent variables, which takes place reducing the motion amplitude. The situation inverts itself passing to mass-center fluctuations. For the unperturbed system we observe RW with  $H=0$ , and for the perturbed ones FBW. In the presence of the external forces, the low-frequency collective motions that imply the mass-center oscillations *cannibalize in a hegemonic way* the remaining configurational motions, according to a typical mechanism for nonlinear systems, as already shown by Fermi-Pasta-Ulam<sup>12</sup>.

We find again the transition to chaos mechanism for the rubber elasticity, that was previously proposed<sup>12</sup>. In such a way it is detailed by identifying the breaking of the high-entropy ergodic behavior of the unperturbed system in the presence of the external force, with few prevailing collective modes. Therefore, the low-entropy system is defined by a low number of degrees-of-freedom in a similar way to the roller formation, to the instability condition in the convective motion of Benard's cells<sup>27</sup> on increasing the control parameter, corresponding to the temperature difference. In our case the external force plays the role of the order parameter. Nevertheless, we observe that the global configurational mobility is invariant as expected at the thermodynamic equilibrium.

## 4 CONCLUSIONS

A class of phenomena exists, which seem to escape the second principle of thermodynamics. They are the complex systems, which give spontaneous phenomena of differentiation and self-organization. For example, in the Couette-Taylor experiment<sup>28</sup>, two coaxial cylinders, containing a liquid are rotated. Above a critical value of applied rotation rate, in the moving liquid ordered and oscillating rolls are generated. A further example is given by the spontaneous formation of simple or complex crystalline structures, as snowflakes<sup>29</sup>. The self-organized processes imply a local entropy decrease, compensated by an increase of the ambient one. In such a way, the formation of dissipative structures occurs with an increase of the global entropy, as required by the second principle. From this point of view, the protein folding itself falls within the class of the self-organized phenomena, and, in the light of the obtained results, also the macromolecular elasticity is

a similar process. For elastomers upon stretching a local decrease of entropy is observed, that can imply also crystallization phenomena (as in synthetic rubbers as polybutadiene or natural as polyisoprene, but not in Protein Rubbers).

In conditions of instability, the symmetric systems show less symmetric behaviors<sup>28</sup>. When the spherical raindrops fall on the flat surface of a lake, they break themselves in crowned spots: from the point of the impact an uniform circular ring rises from the wall which sharpens and curves itself towards outside, breaking itself in a number of tips (in ideal conditions mathematical models indicate 24 tips). The tips, in turn, sharpen themselves towards the top, expelling a rounded small drop. A similar phenomenon is observed during the deformation of a cylinder uniformly compressed along its axis: when the compression reaches a critical load, the undeformed state becomes unstable and the Yoshimura structure<sup>30</sup> appears with symmetrical wrinkle pattern. As well, a sphere compressed by spherically symmetric forces, loses its symmetry deforming itself according to a circular symmetry. And the homogeneous flows generates the Karman vortex street of reduced symmetry behind a circular cylinder<sup>31</sup>.

This is the *mechanism of structure formation by the symmetry breaking*. The typical result of the symmetry breaking is the formation of regular structures in a geometric sense. Only seldom the whole symmetry is lost: the stone which breaks the roto-translational symmetry of the pond generates circular waves that hold the rotation symmetry.

Nevertheless, according to the *extended Curie principle*<sup>28</sup>, the microscopic asymmetries, as the not eliminable thermal fluctuations, play the key role in the choice of the effective final result in the *symmetric ensemble of the possible effects*: the symmetry is more dispersed than lost. In this sense, the sensible dependence upon the initial conditions, typical of the chaotic systems, the breaking of the symmetry of the unstable systems and the second law of thermodynamics combine them. The concept of the symmetry breaking has an enormous interest and is applied in all the sciences, from biology to astronomy.

In the case of the Elastin polypeptide chain, the obtained results show that the unperturbed system presents a symmetrically dynamics of the internal freedom. For the stressed system, the entropy reduction is associated to the symmetry breaking of the chaotic motion: the transition from dynamics, which involves  $3N-6$  degrees-of-freedom to the few collective modes with a large displacement of the mass-center.

This is a phenomenon of symmetry breaking in which, far from equilibrium in instability conditions, the energy equidistribution is lost and the motion is localized in the slower system variables at expense of the faster ones. At a macroscopic level the dynamics is determined by the macroscopic observables, called order parameters (in our case the external elastic force) with an enormous reduction of the degrees-of-freedom, as largely discussed in synergetics<sup>32</sup>. This phenomenology is similar to that observed in the Pasta-Ulam-Fermi problem, where the vibrational

motion of a chain of nonlinear coupled and *end-constrained* oscillators is more localized in low-frequency solitons than distributed according to the energy equipartition, as largely discussed elsewhere<sup>12</sup>.

In our case, the system remaining disordered even under stretching, the transition is not strictly order-disorder or linear-nonlinear like. The observed dynamics is chaotic in all cases, nevertheless under stretching an enormous reduction of the degrees-of-freedom with respect to the nonlinear behavior with a consequent decrease of entropy in Lyapunov sense<sup>14</sup>.

Nevertheless, the global mobility of unperturbed or stretched chains is similar, although due to strongly different effects, according to the classical rubber theory of elasticity. Accordingly, to the described dynamic picture, the slower variables of the constrained chains prevail, under stretching, on the remaining degree-of-freedom of the system.

The *Chaos-Symmetry-Breaking* mechanism, recognized by us for a short flexible chain of a rubber protein, could be generalized to the entropic mechanism of the rubber elasticity.

In the light of the known experimental results and the equations of the classical theories, the entropy change under stretching is proportional to the crosslinks density, then inversely proportional to the crosslinked chain length. This result is in agreement with the proposed mechanism; in fact the extent of the expected effects will depend upon the number of the constrained chains.

The effort of quantifying the free energy changes as a function of the chain length, of the temperature and of the fluctuation amplitude of the unperturbed chain, is in progress.

In such a way, the macromolecular elastic behavior is taken back to the framework of the self-organized behaviors, shown by the complex dynamical systems.

## Acknowledgments

The author acknowledges the CASPUR (Rome, Italy) for the use of the cluster of parallel computers and for AMBER there installed, Dr. G. Chillemi (CASPUR) for having facilitated the execution of the jobs and C.L.Pierri for the collaboration in the present pagination.

## 5 REFERENCES

- 1) M. Rubinstein and S. Panyukov, *Macromolecules* **30**, 8036 (1997)
- 2) H. M. James and E. Guth, *J. Chem. Phys.* **11**, 455 (1943)
- 3) P. J. Flory, *Principles of Polymer Chemistry*, Cornell University Press, Ithaca NY 1953
- 4) G. Allegra, S. Bontempelli and G. Raos, *J. Chem. Phys.* **105**, 8352 (1996)
- 5) Z. R. Wasserman and F. R. Salemme, *Biopolymers* **29**, 1613 (1990)
- 6) B. Li, O. V. Alonso, B. J. Bennion and V. Daggett, *J. Am. Chem. Soc.* **123**, 11991 (2001)
- 7) P. G. de Gennes, *Scaling Concepts in Polymer Physics*, Cornell University Press, Ithaca, 1979, fourth printing 1993
- 8) A. S. Tatham and P. R. Shewry, *Trends Biochem. Sci.* **25**, 567 (2000)
- 9) A. M. Tamburro, V. Guantieri, L. Pandolfo, A. Scopa, *Biopolymers*, **29**, 855 (1990)

- 10) V. Villani and A. M. Tamburro, *J. Chem. Soc., Perkin Trans. 2*, 1951 (1993)
- 11) V. Villani and A. M. Tamburro, *J. Biomol. Struct. Dyn.* **12**, 1173 (1995)
- 12) V. Villani, L. D'Alessio and A. M. Tamburro, *J. Chem. Soc., Perkin Trans. 2*, 2375 (1997)
- 13) V. Villani, A. M. Tamburro, *J. Mol. Struct. (THEOCHEM)*, 431, 205 (1998)
- 14) V. Villani, A. M. Tamburro and J. M. Zaldivar-Comenges, *J. Chem. Soc., Perkin Trans. 2*, 2177 (2000)
- 15) V. Villani and J. M. Zaldivar-Comenges, *Theor. Chem. Acc.* **104**, 290 (2000)
- 16) V. Villani, in *Recent Research Developments in Organic & Bioorganic Chemistry*, S. G. Pandalai (Editor), Transworld Research Network, 2001
- 17) V. Villani, *Recent Res. Devel. Org. Biorg. Chem.* **5**, 27 (2002)
- 18) W. D. Cornell, P. Cieplak, C. I. Bayly, I. R. Gould, K. M. Merz, Jr., D. M. Ferguson, D. C. Spellmeyer, T. Fox, J. M. Caldwell & P. A. Kollman, *J. Am. Chem. Soc.* **117**, 5179 (1995)
- 19) Jorgensen W.L., Chandrasekhar J., Madura J.D., Impey R.W. and Klein M.L., *J. Chem. Phys.*, **79**, 926 (1983)
- 20) Berendsen H.J.C., Postma J.P.M., van Gunsteren W.F., Di Nola A. and Haak J.R., *J. Chem. Phys.* **81**, 3684 (1984)
- 21) L. Verlet, *Phys. Rev.*, **159**, 98, 1967
- 22) Mandelbrot B.B., *The Fractal Geometry of Nature*, W.H. Freeman, New York 1982
- 23) D. A. Case, D. A. Pearlman, J. W. Caldwell, T. E. Cheatham III, W. R. Ross, C. Simmerling, T. Darden, K. M. Merz, R. V. Stanton, A. Cheng, J. J. Vincent, M. Crowley, V. Tsui, R. Radmer, Y. Duan, J. Pitera, I. Massova, G. L. Seibel, U.C. Singh, P. Weiner, P. A. Kollman, AMBER 6, University of California, San Francisco, 1999
- 24) <http://www.trusoft.netmegs.com/benoit.html>
- 25) R. Hegger, H. Kantz, and T. Schreiber, *Practical implementation of nonlinear time series methods: The TISEAN package*, *CHAOS* **9**, 413 (1999) P. Bak, C. Tang & K. Wiesenfeld, *Phys. Rev. Lett.* **59**, 381 (1987)
- 26) S. Carrà, *La formazione delle strutture*, Bollati Boringhieri, Torino, 1989
- 27) I. Stewart and M. Golubitsky, *Fearful Symmetry. Is God a Geometer?*, Blackwell, London, 1992
- 28) I. Stewart, *What Shape is a Snowflake*, Weidenfeld & Nicolson, London, 2001
- 29) I. Stewart, *Les symétries de la Nature*, Dossier de 'Pour la Science', n. 20, luglio 1998
- 30) M. Van Dyke, *An Album of Fluid Motion*, The Parabolic Press, Stanford, 1982
- 31) H. Haken, *Erfolgsgeheimnisse der Natur*, Deutsche Verlags-Anstalt, Stoccarda, 1981

## Biography

Vincenzo Villani, born in 1959, is researcher in Macromolecular Chemistry at the University of Basilicata (Italy). He is professor of *Theory of Macromolecules* and group leader. Graduate at University of Naples, he is author of about 60 scientific publications. He has developed models of catalytic sites in the Ziegler-Natta isospecific polymerization. He has investigated of drug design at a semiempiric and *ab-initio* level. He has developed methods of conformational search and of simulated annealing of complex molecular systems. He has studied the dynamics of biomolecules in aqueous solution using the time series nonlinear analysis. He has proposed an entropic mechanism and a model morphology for the Protein Rubbers within the theory of complex systems. He is involved in epistemology and in science diffusion (<http://www.unibas.it/utenti/villani/index.htm>).